North Pacific Fisheries Commission

NPFC-2021-SCsm01-WP02

Updated stock assessment of Pacific saury (*Cololabis saira*) in the Western North Pacific Ocean through 2019

Jhen Hsu[1], Yi-Jay Chang[1], Chih-hao Hsieh[1], Wen-Bin Huang[2], Tung-Hsieh Chiang[3]

1. Institute of Oceanography, National Taiwan University

2. Department of Natural Resources and Environmental Studies, National Dong Hwa University

3. Overseas Fisheries Development Council of Chinese Taipei

Summary

This paper describes the updated stock assessment of the Pacific saury (*Cololabis saira*) in the Western North Pacific Ocean (WNPO) based on the guideline of the 2019 SSC PS05. The assessment consisted of applying the Bayesian state-space surplus production model for estimating the biomass from 1980 to 2019 with available catches from 1980 to 2019. Abundance indices available for WNPO Pacific saury consisted of standardized catch-per-unit-effort (CPUE) of stick-held dip net fisheries from Japan (1980 – 2019), Chinese Taipei (2001 – 2019), Russia (1994 – 2019), Korea (2001 – 2019), and China (2013 – 2019), and biomass survey from Japan (2003 – 2019). Two base case models were considered for the assessment outputs. The results of two base case models indicated that the estimated biomass trends before 2000 were sensitive to the early Japanese CPUE index (1980 – 1993). The ensemble time-series of biomass is estimated to have an increasing pattern since 2000 with the peaks in 2005 and 2008, after then dramatically decreased overtime and below B_{MSY} in 2015 – 2019. It should be noted that the models estimate an increase in biomass in 2018 (median B_{2018}/B_{MSY} = 0.80, 80 percentile range 0.56 – 1.20) and following a slightly decrease in 2019 (median B_{2019}/B_{MSY} = 0.56, 80 percentile range 0.39 – 0.84). A steady increase in fishing mortality is estimated to have occurred from 2004 to 2018, but a substantial decrease in fishing mortality was estimated in 2019 (median F_{2019}/F_{MSY} = 0.82, 80 percentile range 0.45 – 1.38). The recent average fishing mortality is estimated to be above F_{MSY} (median $F_{2017\text{-}2019}/F_{MSY}$ = 1.28, 80 percentile range 0.66 – 2.49). The ensemble MCMC results from the two base cases indicated that the 2019 stock status is likely within the yellow quadrant (Prob[$B_{2019}<B_{MSY}$ and $F_{2019}<F_{MSY}$] = 61.35%).

1. Introduction

Here, we present an updated stock assessment of Pacific saury in the WNPO of the North Pacific Fisheries Commission (NPFC) convention area. The assessment consisted of applying the

Bayesian state-space surplus production model with available catches and standardized catch-per-unit-effort (CPUE) indices from the members from 1980 to 2019 and the Japanese biomass index from 2003-2019. The Bayesian method provided the direct estimates of uncertainty of the model parameters and management quantities. The objectives of this study are to conduct a stock assessment for the Pacific saury in the WNPO through 2019, to examine the sensitivity of the results to changes in model structural uncertainty, to determine the ensemble stock condition from the developed base cases. Since the SSC PS agreed to not conduct the stock projections due to the poor predictive ability of the current Bayesian surplus production model (NPFC-2020-SSC PS06-Final Report), therefore we did not include the stock projection and its risk analysis in this updated stock assessment report.

2. Material and methods

Fishery catch data from 1950 – 2019 for assessing WNPO saury were taken from the most recent summary of available fishery-dependent data (NPFC-2019-SSC PS05-Final Report). The commercial catch of Pacific saury caught by Japan, Chinese Taipei, Korea, China, Russia and other members in the WNPO area were collected from 1950 to 2019 (**Figure 1**). Estimates of standardized fishery-dependent catch-per-unit-effort (CPUE) of WNPO saury were available for Japanese offshore stick-held dip net fisheries, however, Japanese standardized CPUE data was separated into two time series, one before 1994 (1980 – 1993) (NPFC-TWG PSSA03-WP11) and one from 1994 to 2019 (NPFC-2020-SSC-PS06-WP12) to account for the potential change in catchability. Indices of Chinese Taipei and Korean distant-water stick-held dip net fisheries were available from 2001 – 2019 (NPFC-2020-SSC PS06-WP05 and NPFC-2020-SSC PS06-WP03). Russia provided the abundance index of offshore and distant stick-held dip net fisheries from 1994 – 2019 (NPFC-2020-SSC PS06-WP04). Index of Chinese distant-water stick-held dip net fisheries was also available from 2013-2019 (NPFC-2020-SSC PS06-WP07). Fishery-independent biomass index was available from Japanese scientific research surveys from 2003 – 2019 by using mid-water trawl (NPFC-2019-SSC PS05-WP08) (**Figure 2**).

Based on the SSC PS05 recommended base case scenarios (NPFC-2019-SSC PS05-Final Report), two models differed in the inclusion of the early Japanese CPUE, and the observation error variance of the CPUEs were explored (**Table 1**). We also developed four sensitivity cases (**Table 1**) to evaluate the model outputs of the base cases following the recommendation of the SSC PS05 (NPFC-2019-SSC PS05-Final Report).

The Bayesian analysis requires prior probability distributions for each of the model parameters. These priors were summarized in **Table 2**.

3. Results

3.1 Convergence of base case model

The visual inspection of trace plots of the major parameters showed the good mixing of the three chains (i.e., moving around the parameter space), also indicative of convergence of the MCMC chains. The Gelman and Rubin statistic for all parameters, including all variance terms, equalled 1, which indicated convergence of the Markov chains. Similarly, the Heidelberger and Welch test could not reject the hypothesis that the MCMC chains were stationary at the 95% confidence level for any of the parameters. Overall, these diagnostics indicated that the posterior distributions of the model parameters were adequately sampled with the MCMC simulations.

3.2 Model fits to catch-per-unit-effort indices

Plots of residual diagnostics by fishery for the base case models were shown in **Figures S1** – **S2**. Models fit to the Chinese Taipei index had a residual trend with negative residuals in 2002 – 2010 and positive residuals in 2011 – 2019. Overall, the model fits to the WNPO Pacific saury indices indicated that there was a lack of fit to the Chinese Taipei CPUE.

3.3 Posterior estimates of model parameters

Plots of posterior densities of the parameters r, K, M, σ^2, τ^2, β, and P_1 for each base case were shown in **Figures S3** – **S4**, together with their respective prior densities. Similar to the log-normal priors, the marginal posteriors generally have a long right-hand tail in the density plot. Summaries of posterior medians of parameters of the base cases were provided in **Tables S1** – **S3**. The results of time-varying catchability (q) in early Japanese CPUE (1980 – 1993) were shown in **Figure S5** and **Table S1**.

3.4 Stock assessment results

Time-series of biomass (B), biomass depletion (B/K) and the ratio of biomass to B_{MSY} (B/B_{MSY}) within each base case and sensitivity case were provided in **Figure 3a – c** and **Figure S6 – S11**, respectively. Different trends in biomass during 1980 – 1987 were found between base case 1 and base case 2. However, the biomass trends after 2000 were consistent between the two base cases. The ensemble time-series of biomass is estimated to have an increasing pattern since 2000 with the peaks in 2005 and 2008, after then dramatically decreased overtime and below B_{MSY} in 2015 – 2019. It should be noted that the models estimate an increase in biomass in 2018 (median B_{2018}/B_{MSY} = 0.80, 80 percentile range 0.56 – 1.20) and following a slightly decrease in 2019 (median B_{2019}/B_{MSY} = 0.56, 80 percentile range 0.39 – 0.84).

Time-series of the ratio of fishing mortality to (F/F_{MSY}) within two base cases and four sensitivity cases were provided in **Figure 3d** and **Figure S12 – S17**, respectively. Differences in trends for the ratio of fishing mortality during 1980 – 1993 were found between base cases 1 and 2. Since 1994, there were similar trends among the two base case models. The ensemble time-series of fishing mortality ratio trend from two base cases were shown in **Figure 3d**. A steady increase in fishing mortality is estimated to have occurred from 2004 to 2018 and the recent average fishing mortality is estimated to be above F_{MSY} (median $F_{2017\text{-}2019}/F_{MSY}$ = 1.28, 80 percentile range 0.66 – 2.49). It should be noted that

the models estimate a substantial decrease in fishing mortality in 2019 (median F_{2019}/F_{MSY} = 0.82, 80 percentile range 0.45 – 1.38).

The quantities of management interest reference points from joint estimates of the base cases 1 and 2 were shown in **Table 3,** and each of the base cases was shown in **Tables S4** and **S5,** respectively. Overall, the ensemble MCMC results from the two base cases indicated that the 2019 stock status is likely within the yellow quadrant (Prob [$B_{2019}<B_{MSY}$ and $F_{2019}<F_{MSY}$] = 65.01%) (**Figure 4**).

3.5 Retrospective analysis

Retrospective analyses show that the time-series of B/B_{MSY} and F/F_{MSY} estimated by each of the base cases with the removal of the most 6 years of data (2014 – 2019) in successive model runs generally match well with the full-time series assessment (**Figures S20 – S21**). This suggested that there is no consistent pattern of bias in the estimates of B/B_{MSY} and F/F_{MSY}.

Table 1. Specifications of the two base case models and four sensitivity case models. “JPN_early” = early Japan (1980 – 1993), “JPN_late” = late Japan (1994 – 2019), “CT” = Chinese Taipei, “RUS” = Russia, “KOR” = Korea, “CHN” = China, “JPN_bio” = Japan biomass survey. $q1$ = fishing efficiency of the Japanese mid-water trawl net; q = generic catchability of the Japanese biomass survey.

	Base case 1	Base case 2	Sensitivity case 1 & 2	Sensitivity case 3 & 4
Initial year	1980		1980	1980/2001
Biomass survey	B_obs = B_est*$q1$ ~ LN(log(q*B), σ^2) q~U(0, 1)		q~U(0, 2)	q~U(0, 1) 2003-2019
CPUE	CHN (2013-2018) JPN_early (1980-1993; with time-varying q) JPN_late (1994-2019) KOR (2001-2019) RUS (1994-2019) CT (2001-2019)	CHN (2013-2019) JPN_late (1994-2019) KOR (2001-2019) RUS (1994-2019) CT (2001-2019)	Two sets as on the left for sensitivity case 1 and 2 respectively	Sensitivity case 3: Joint CPUE (2001-2019) Sensitivity case 4: Joint CPUE (2001 – 2019) and JPN_early with time-varying q
Variance component	6 times of biomass	5 times of biomass	Same as base cases 1 and 2, respectively	Same weight between biomass and joint CPUE
Hyper-depletion/ stability	β ~ U(0, 1) but [β_JPN_early=1]	β ~ U(0, 1)	Same as base cases 1 and 2, respectively	b ~ U(0, 1)

Table 2. Summary of the specified priors for the Bayesian state-space models. “JPN1” = early Japan (1980 – 1993), “JPN2” = late Japan (1994 – 2019), “CT” = Chinese Taipei, “RUS” = Russia, “KOR” = Korea, “CHN” = China, “JPN_bio” = Japan biomass survey.

Parameter	Description	Prior
K	Carrying capacity (10,000 mt)	$K \sim \log N\left(\log(150) - \frac{\sigma_K^2}{2}, \sigma_K^2\right); CV_K = 1$
r	Intrinsic growth rate (year^{-1})	$r \sim \log N\left(\log(1.4) - \frac{\sigma_r^2}{2}, \sigma_r^2\right); CV_r = 2$
M	Shape parameter	$M \sim \text{Gamma}(2,2)$
q	Catchability for others fleets (JPN2;CT; RUS; KOR and CHN)	$1/q \sim \text{Gamma}(0.01, 0.01)$
q_{bio}	Catchability for Japanese survey biomass	$q_{bio} \sim \text{Uniform}(0,1)$
q_{JPN1}^{1980}	Time-varying catchability for JPN1 in 1980	$q_{JPN1}^{1980} \sim \text{Uniform}(1\times10^{-7}, 2)$
ω	Annual deviations of the log-scale time-varying catchability	$\omega \sim N(0, 0.1)$
β	Hyperstability of 1994-2019	$\beta \sim \text{Uniform}(0,1)$
σ^2	Common observation error of CPUE	$1/\sigma^2 \sim \text{Gamma}(2, 0.45); CV_\tau = 1$
τ^2	Process error	$1/\tau^2 \sim \text{Gamma}(4, 0.1)$
P_1	Initial condition (B_1/K)	$P_1 \sim \log N\left(\log(0.7) - \frac{\sigma_{P_1}^2}{2}, \sigma_{P_1}^2\right); CV_{P_1} = 1$

$CV_\theta = \left(\exp\left(\sigma_\theta^2\right) - 1\right)^{1/2}$

Table 3. Summary of joint estimates of reference points of the base cases 1 and 2.

	Mean	Median	Lower 10th	Upper 10th
C_{2019}	19.2	19.2	19.2	19.2
$Ave\_C_{2017\text{-}2019}$	29.8	29.8	29.8	29.8
$Ave\_F_{2017\text{-}2019}$	0.891	0.523	0.21	1.517
F_{2019}	0.455	0.346	0.145	0.812
F_{MSY}	0.494	0.435	0.231	0.794
MSY	42.00	41.11	34.03	50.98
F_{2019}/F_{MSY}	0.891	0.824	0.45	1.376
$Ave\_F_{2017\text{-}2019}/F_{MSY}$	1.56	1.282	0.664	2.491
K	280.352	252.4	160.2	435.51
B_{2018}	114.44	93.24	50.4	202.2
B_{2019}	80.319	65.7	34.6	143
$Ave\_B_{2017\text{-}2019}$	89.262	73.258	39.683	156.733
B_{MSY}	130.559	117	75.409	202.1
B_{MSY}/K	0.508	0.46	0.294	0.746
B_{2018}/K	0.393	0.377	0.262	0.543
B_{2019}/K	0.275	0.266	0.182	0.38
$Ave\_B_{2017\text{-}2019}/K$	0.307	0.297	0.209	0.416
B_{2018}/B_{MSY}	0.848	0.798	0.558	1.202
B_{2019}/B_{MSY}	0.593	0.563	0.387	0.838
$AveB_{2017\text{-}2019}/B_{MSY}$	0.661	0.626	0.446	0.921

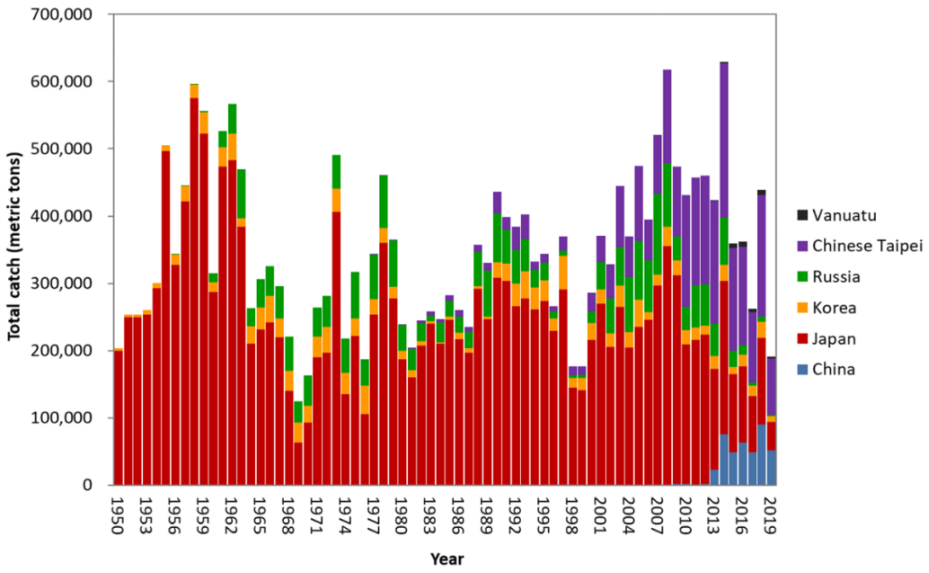

Figure 1. Time-series of catches (metric ton) of the Pacific saury in the Western North Pacific Ocean from 1950 to 2019 by the members.

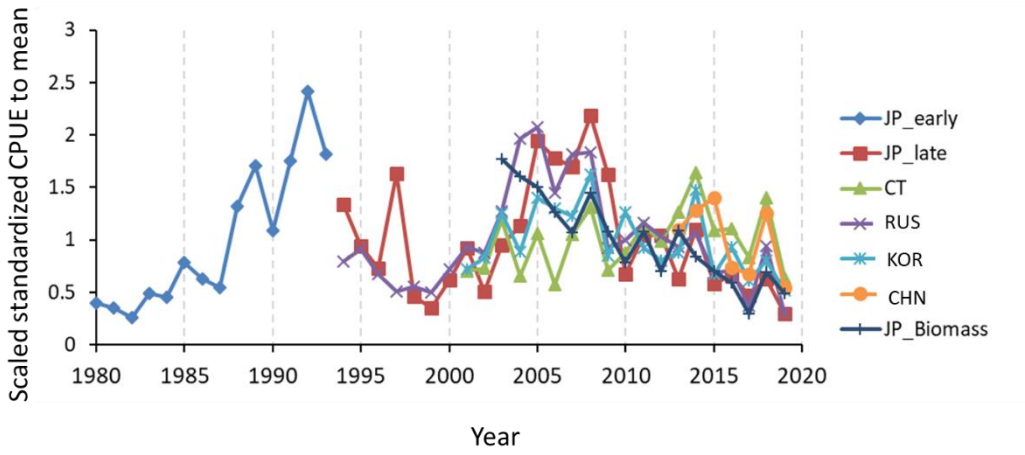

Figure 2. Pacific saury CPUE indices from early Japan (JPN_early), late Japan (JPN_late), Chinese Taipei (CT), Russia (RUS), Korea (KOR), and China (CHN) stick-held dip net fisheries, and biomass survey index of Japan (JP_Biomass) during 1980 – 2019 in the Western North Pacific Ocean.

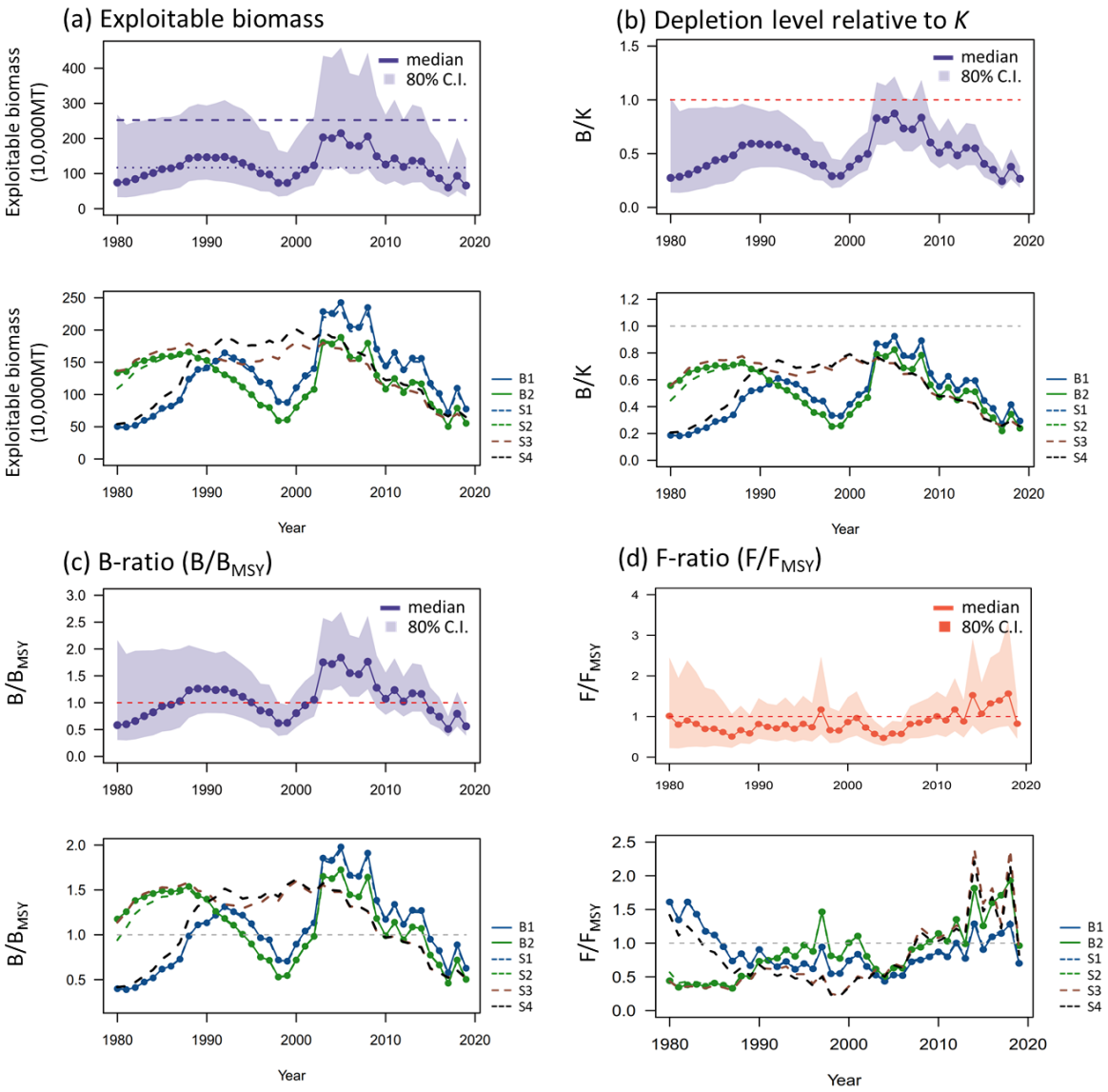

Figure 3. Time series of ensemble biomass (10,000 metric ton) (a), depletion ratio (B/K) (b), the ratio of biomass to B_{MSY} (B/B_{MSY}) (c), and the ratio of fishing mortality to F_{MSY} of the Western North Pacific saury for the median estimates of MCMC results from base cases 1 – 2 and sensitivity cases 1 – 4. In panel (a), the upper dashed and lower dotted horizontal line denotes the carrying capacity (K) and BMSY, respectively. In panels (b) and (c), the dashed lines denote the reference levels of 1.

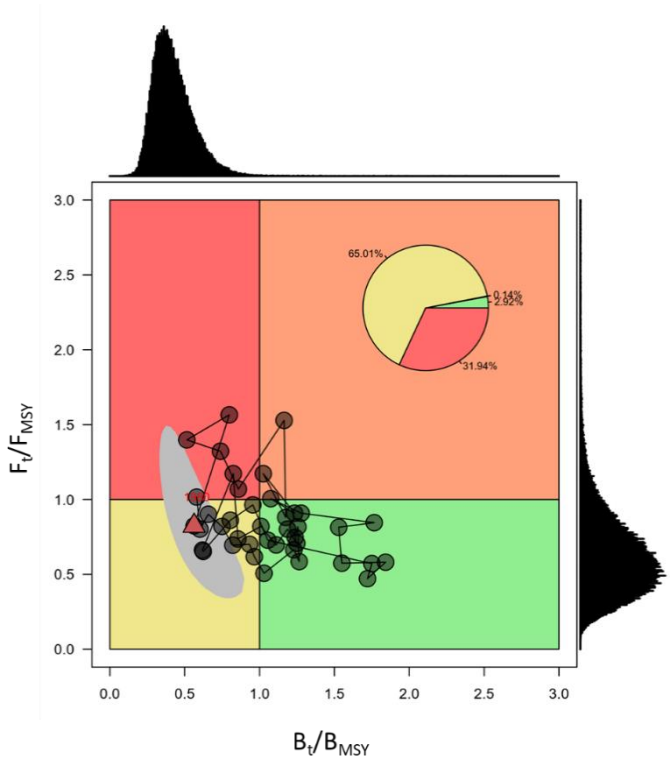

Figure 4. Ensemble Kobe phase plot of the stock trajectory of the Western North Pacific saury from 1980 to 2019 (in red triangle) with uncertainty estimate in 2019 (80% credible intervals, grey polygon) from the two base case models.

Supplementary

Table S1. Summary of parameter estimates of the base case 1.

	Mean	Median	Lower 10th	Upper 10th
r	1.107	0.91	0.465	1.934
K	297.372	269.8	176.5	455
q_{CHN}	0.178	0.162	0.083	0.295
q_{JPN2}	0.023	0.021	0.011	0.038
q_{KOR}	0.236	0.215	0.112	0.388
q_{RUS}	0.107	0.098	0.05	0.175
q_{CT}	0.023	0.021	0.011	0.038
q_{Bio}	0.39	0.362	0.175	0.65
Shape parameter (*M*)	0.725	0.618	0.247	1.338
observation error (σ_{com})	0.34	0.339	0.308	0.375
observation error (σ_{bio})	0.14	0.14	0.127	0.154
process error(τ)	0.228	0.225	0.176	0.284
F_{MSY}	0.448	0.415	0.237	0.699
B_{MSY}	137.584	124.2	82.12	210
MSY	43.119	41.84	35.03	52.79
b	0.915	0.92	0.848	0.978
*q*_JPN1_1980	0.0146	0.0134	0.0069	0.0238
*q*_JPN1_1981	0.0144	0.0133	0.0069	0.0234
*q*_JPN1_1982	0.0144	0.0133	0.0069	0.0232
*q*_JPN1_1983	0.0149	0.0138	0.0071	0.0240
*q*_JPN1_1984	0.0153	0.0141	0.0074	0.0248
*q*_JPN1_1985	0.0160	0.0148	0.0078	0.0258
*q*_JPN1_1986	0.0164	0.0151	0.0080	0.0264
*q*_JPN1_1987	0.0169	0.0156	0.0083	0.0272
*q*_JPN1_1988	0.0180	0.0167	0.0089	0.0290
*q*_JPN1_1989	0.0191	0.0176	0.0094	0.0307
*q*_JPN1_1990	0.0198	0.0182	0.0097	0.0319
*q*_JPN1_1991	0.0211	0.0194	0.0103	0.0341
*q*_JPN1_1992	0.0223	0.0205	0.0108	0.0361
*q*_JPN1_1993	0.0231	0.0212	0.0110	0.0377

Table S2. Summary of parameter estimates of the base case 2.

	Mean	Median	Lower 10th	Upper 10th
r	1.143	0.947	0.443	2.042
K	263.331	234.2	149.1	414.41
qCHN	0.586	0.509	0.233	1.032
qJPN2	0.082	0.071	0.032	0.145
qKOR	0.818	0.71	0.32	1.455
qRUS	0.37	0.321	0.145	0.66
qCT	0.08	0.069	0.031	0.142
qBio	0.513	0.483	0.229	0.832
shape parameter (*M*)	0.79	0.676	0.269	1.453
observation error (σ_{com})	0.344	0.342	0.31	0.38
observation error (σ_{bio})	0.154	0.153	0.139	0.17
process error (τ)	0.25	0.245	0.185	0.321
F_{MSY}	0.54	0.462	0.224	0.895
B_{MSY}	123.534	109.5	70.499	193.31
MSY	40.882	40.35	33.04	49
b	0.719	0.718	0.583	0.861

Table S3. Summary of joint estimates of model parameters of the base cases 1 and 2.

	Mean	Median	Lower 10th	Upper 10th
r	1.125	0.927	0.455	1.988
K	280.35	252.40	160.20	435.51
qCHN	0.382	0.268	0.104	0.821
qJPN2	0.052	0.035	0.014	0.115
qKOR	0.527	0.359	0.140	1.148
qRUS	0.239	0.162	0.063	0.521
qCT	0.051	0.035	0.014	0.112
qBio	0.452	0.417	0.195	0.755
shape parameter (*M*)	0.757	0.645	0.258	1.400
observation error (σ_{com})	0.342	0.340	0.309	0.377
observation error (σ_{bio})	0.147	0.146	0.131	0.165
process error (τ)	0.239	0.233	0.180	0.304
F_{MSY}	0.494	0.435	0.231	0.794
B_{MSY}	130.559	117.000	75.409	202.100
MSY	42.000	41.110	34.030	50.980
b	0.817	0.853	0.627	0.962

Table S4. Summary of reference points of the base case 1.

	Mean	Median	Lower 10th	Upper 10th
C_{2019}	19.2	19.2	19.2	19.2
Ave_$C_{2017\text{-}2019}$	29.8	29.8	29.8	29.8
Ave_$F_{2017\text{-}2019}$	0.57	0.42	0.18	1.01
F_{2019}	0.34	0.29	0.13	0.61
F_{MSY}	0.45	0.42	0.24	0.70
MSY	43.12	41.84	35.03	52.79
F_{2019}/F_{MSY}	0.75	0.70	0.40	1.15
Ave_$F_{2017\text{-}2019}/F_{MSY}$	1.18	1.05	0.58	1.83
K	297.37	269.80	176.50	455.00
B_{2018}	131.43	109.60	59.84	228.91
B_{2019}	92.42	77.47	42.00	161.10
Ave_$B_{2017\text{-}2019}$	102.91	86.41	47.66	178.53
B_{MSY}	137.58	124.20	82.12	210.00
B_{MSY}/K	0.47	0.46	0.41	0.53
B_{2018}/K	0.43	0.42	0.29	0.58
B_{2019}/K	0.30	0.29	0.21	0.40
$B_{2017\text{-}2019}/K$	0.33	0.33	0.23	0.44
B_{2018}/B_{MSY}	0.93	0.89	0.62	1.29
B_{2019}/B_{MSY}	0.65	0.63	0.44	0.89
$B_{2017\text{-}2019}/B_{MSY}$	0.73	0.70	0.50	0.98

Table S5. Summary of reference points of the base case 2.

	Mean	Median	Lower 10th	Upper 10th
C_{2019}	19.20	19.20	19.20	19.20
Ave_$C_{2017\text{-}2019}$	29.80	29.80	29.80	29.80
Ave_$F_{2017\text{-}2019}$	1.22	0.67	0.26	2.87
F_{2019}	0.57	0.43	0.18	0.99
F_{MSY}	0.54	0.46	0.22	0.90
MSY	40.88	40.35	33.04	49.00
F_{2019}/F_{MSY}	1.03	0.96	0.55	1.54
$F_{2017\text{-}2019}/F_{MSY}$	1.94	1.57	0.85	3.42
K	263.33	234.20	149.10	414.41
B_{2018}	97.45	78.72	45.21	168.50
B_{2019}	68.22	55.16	30.65	118.30
Ave_$B_{2017\text{-}2019}$	75.61	61.64	35.43	129.60
B_{MSY}	123.53	109.50	70.50	193.31
B_{MSY}/K	0.47	0.47	0.41	0.54
B_{2018}/K	0.36	0.34	0.25	0.49
B_{2019}/K	0.25	0.24	0.17	0.34
$B_{2017\text{-}2019}/K$	0.28	0.27	0.20	0.37
B_{2018}/B_{MSY}	0.77	0.72	0.53	1.07
B_{2019}/B_{MSY}	0.54	0.50	0.36	0.74
$B_{2017\text{-}2019}/B_{MSY}$	0.60	0.56	0.42	0.81

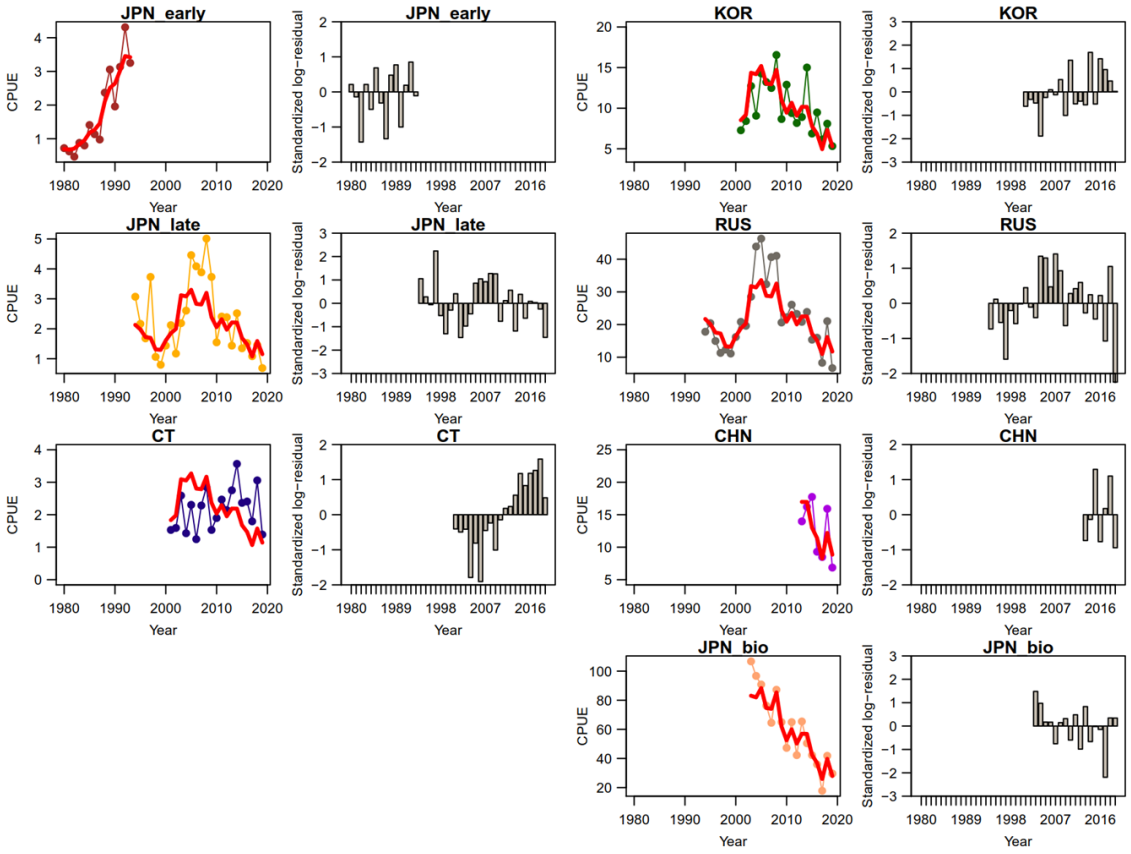

Figure S1. Time-series of observed (circle-line) and predicted (red solid line) catch per unit effort (CPUE) of Western North Pacific saury and standardized log-residuals for the base case 1 production model. “JPN_early” = early Japan (1980-1993), “JPN_late”=late Japan (1994-2019), “CT” = Chinese Taipei, “RUS” = Russia, “KOR”= Korea, “CHN”=China, JPN_bio” = Japanese biomass survey.

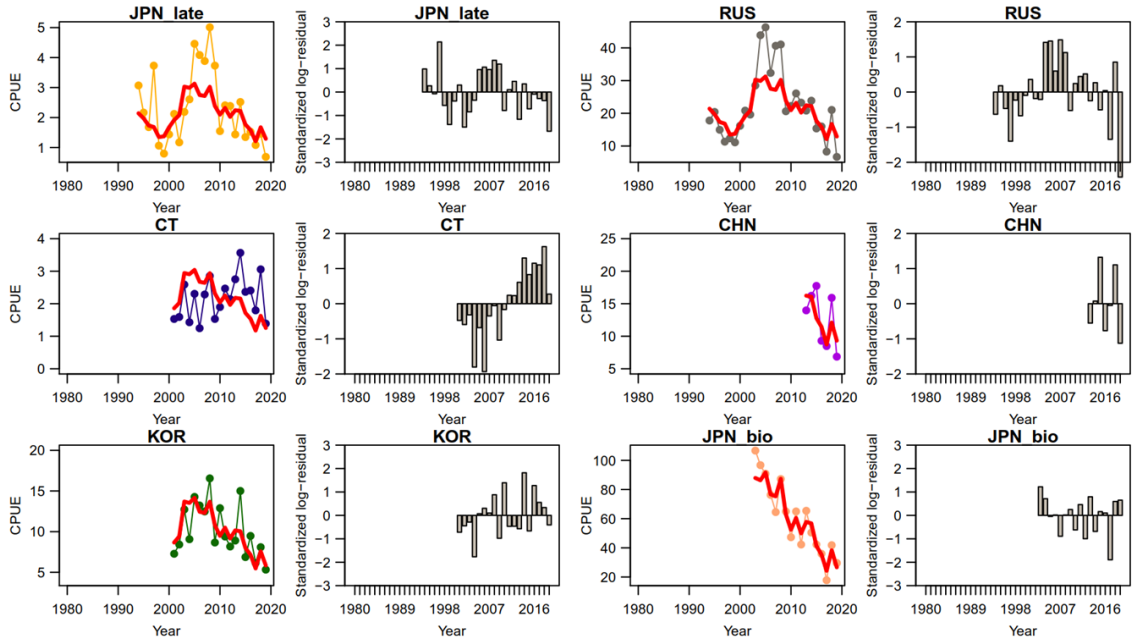

Figure S2. Time-series of observed (circle-line) and predicted (red solid line) catch per unit effort (CPUE) of Western North Pacific saury and standardized log-residuals for the base case 2 production model. “JPN_late”=late Japan (1994-2019), “CT” = Chinese Taipei, RUS” = Russia, “KOR”= Korea, “CHN”=China, “JPN_bio” = Japanese biomass survey.

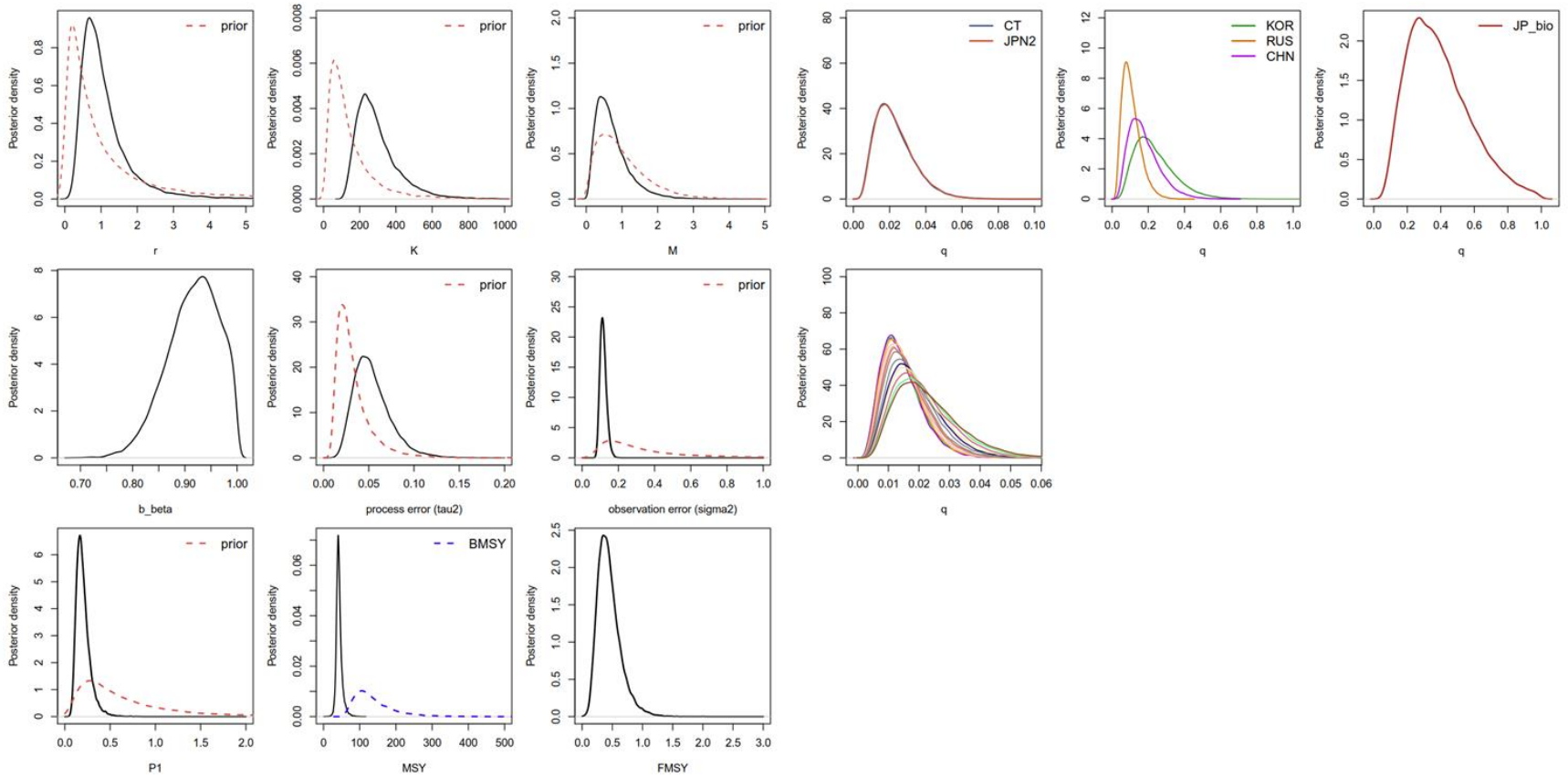

Figure S3. Kernel density estimates of the posterior distributions (solid lines) of various model parameters and management quantities for the base case 1 production model for the Pacific saury in the Western North Pacific Ocean. Proper prior densities are given by the dashed lines. “JPN2”=late Japan (1994-2019), “CT” = Chinese Taipei, “RUS” = Russia, “KOR”= Korea, “CHN”=China, “JP_bio” = Japanese biomass survey.

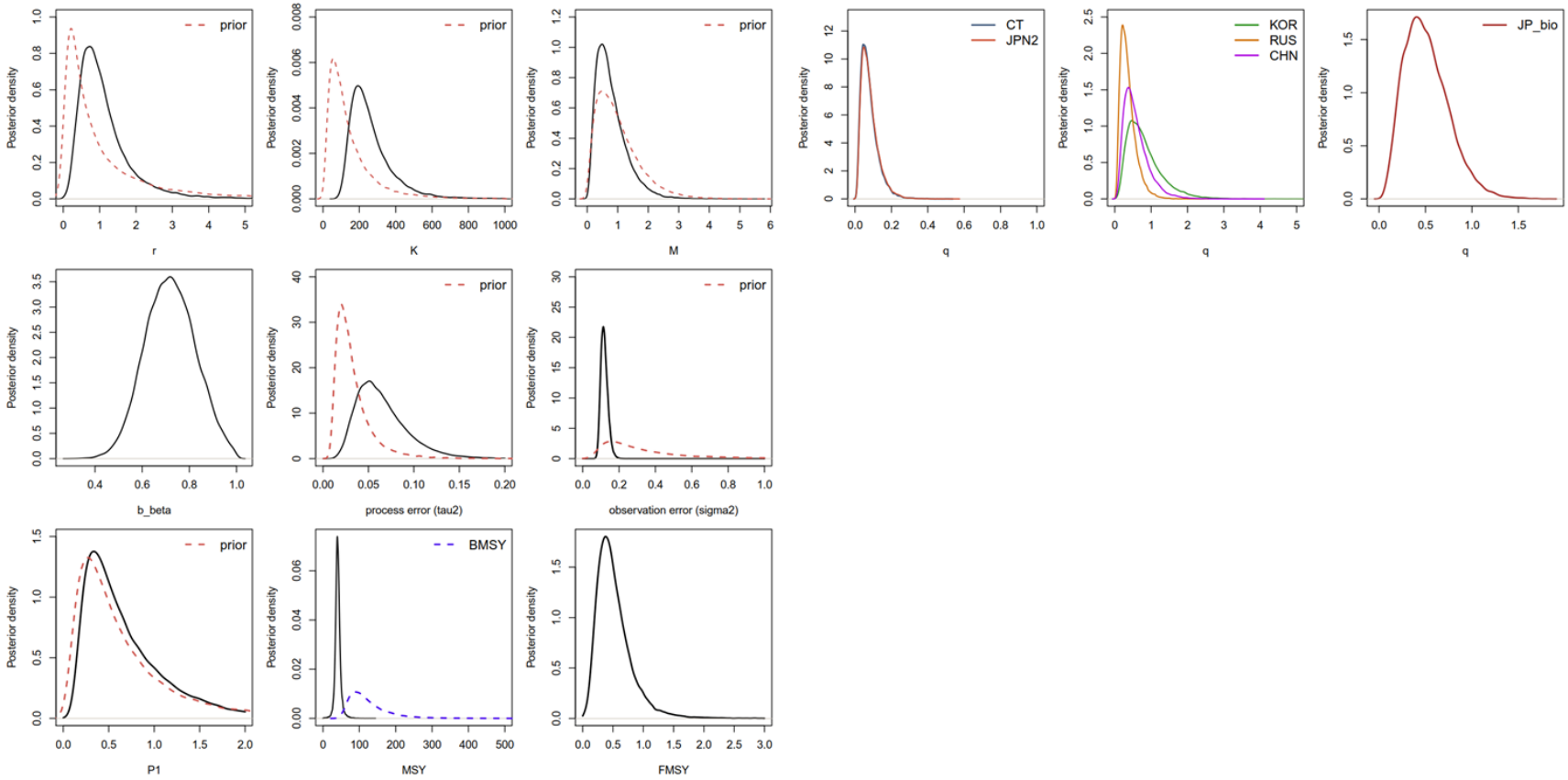

Figure S4. Kernel density estimates of the posterior distributions (solid lines) of various model parameters and management quantities for the base case 2 production model for the Pacific saury in the Western North Pacific Ocean. Proper prior densities are given by the dashed lines. “JPN2”=late Japan (1994-2019), “CT” = Chinese Taipei, “RUS” = Russia, “KOR”= Korea, “CHN”=China, “JP_bio” = Japanese biomass survey.

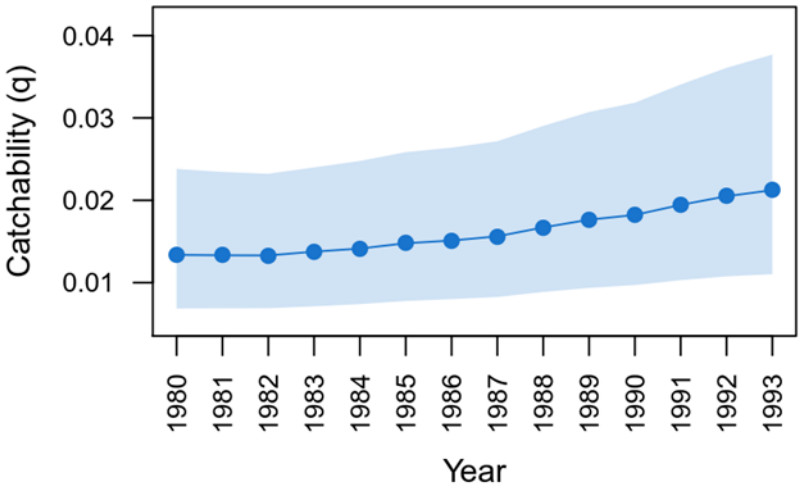

Figure S5. Time series estimates of annual catchabilities of the early Japanese CPUE from 1980 to 1993 for the base case 1.

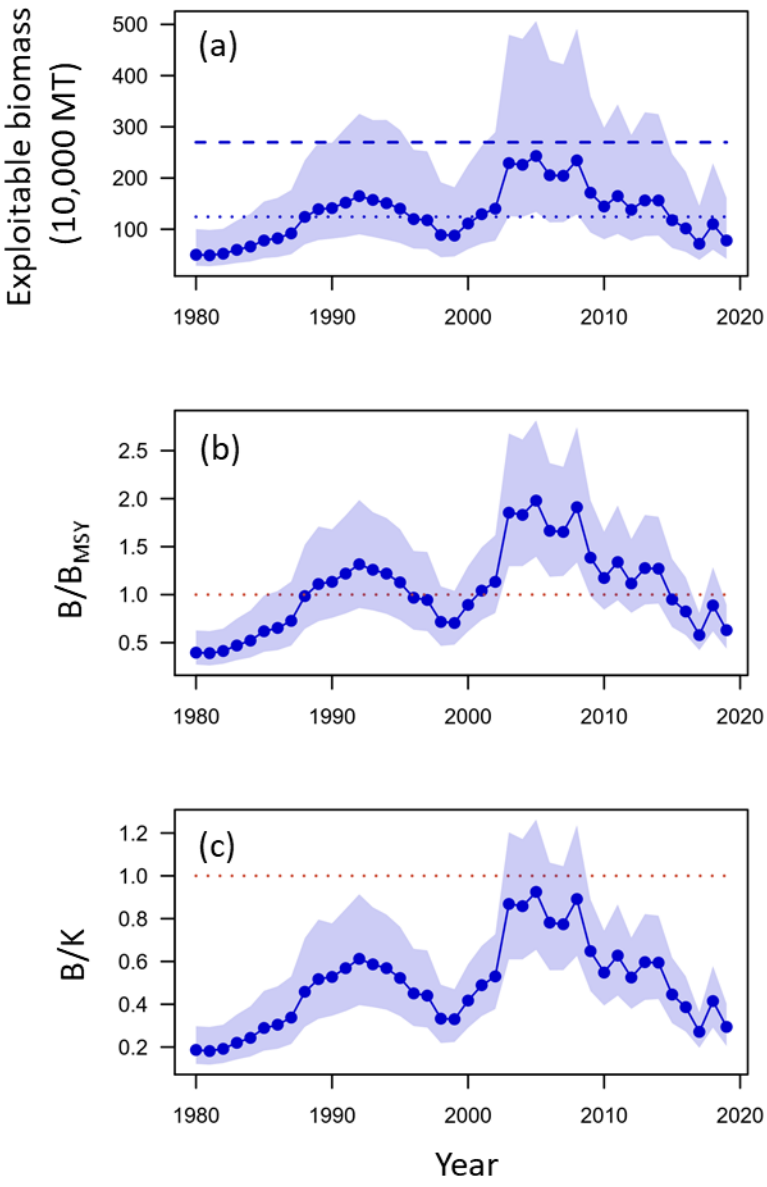

Figure S6. Time series of biomass (10,000 metric ton) (a), ratio of biomass to B_{MSY} (B/B_{MSY}) (b), and depletion ratio (B/K) of the Western North Pacific saury for the base case 1. In panel (a), the upper dashed and lower dotted horizontal line denotes the carrying capacity (K) and B_{MSY}, respectively. In panels (b) and (c), the dashed lines denote the reference levels of 1.

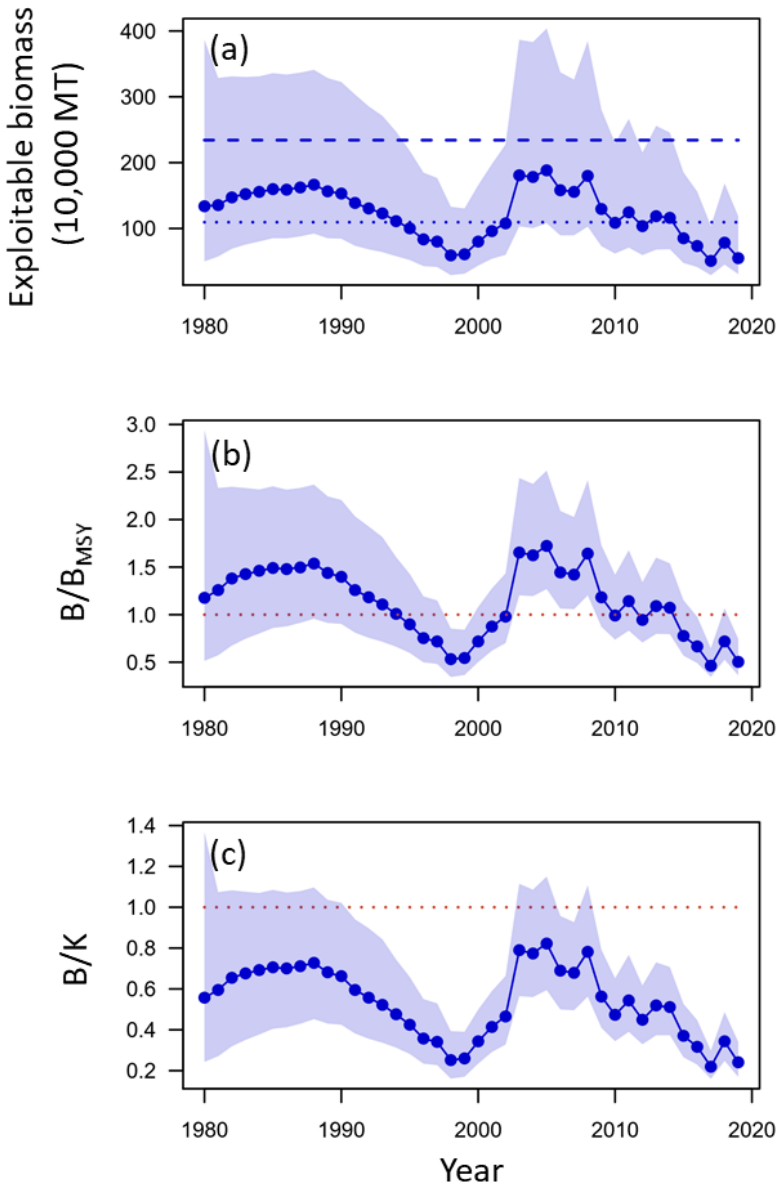

Figure S7. Time series of biomass (10,000 metric ton) (a), ratio of biomass to B_{MSY} (B/B_{MSY}) (b), and depletion ratio (B/K) of the Western North Pacific saury for the base case 2. In panel (a), the upper dashed and lower dotted horizontal line denotes the carrying capacity (K) and B_{MSY}, respectively. In panels (b) and (c), the dashed lines denote the reference levels of 1.

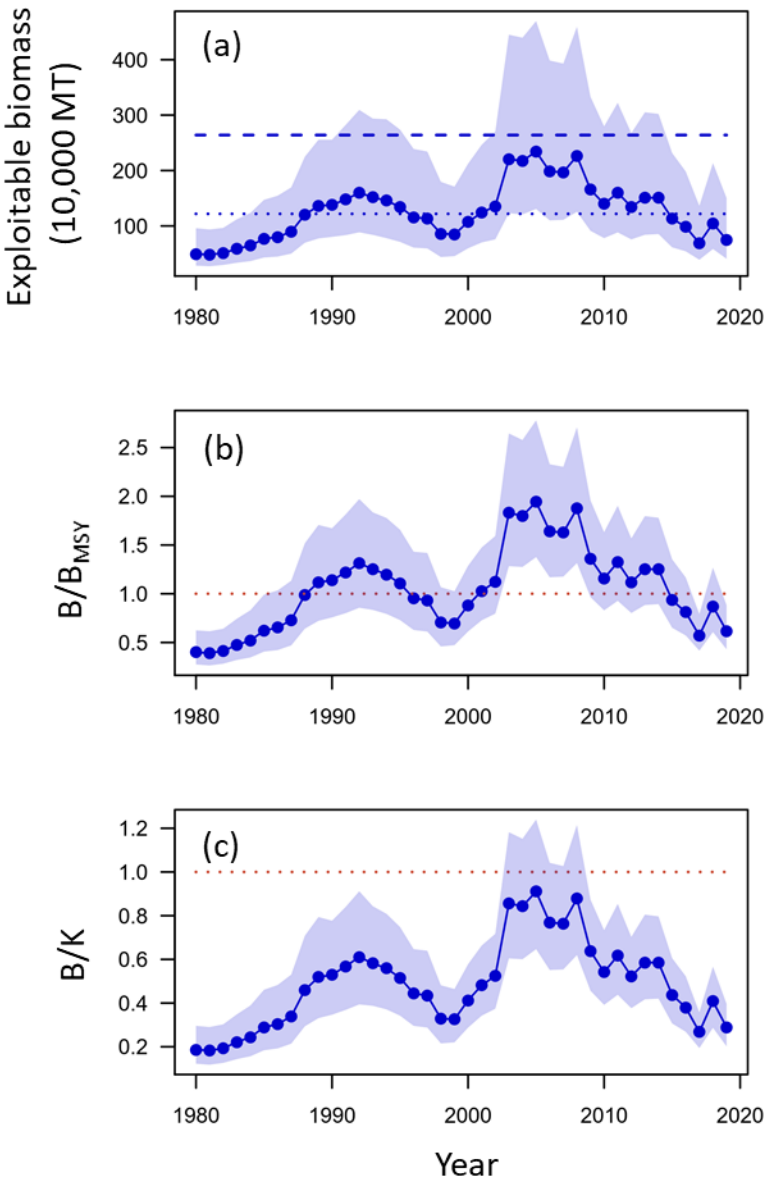

Figure S8. Time series of biomass (10,000 metric ton) (a), ratio of biomass to B_{MSY} (B/B_{MSY}) (b), and depletion ratio (B/K) of the Western North Pacific saury for the sensitivity case 1. In panel (a), the upper dashed and lower dotted horizontal line denotes the carrying capacity (K) and B_{MSY}, respectively. In panels (b) and (c), the dashed lines denote the reference levels of 1.

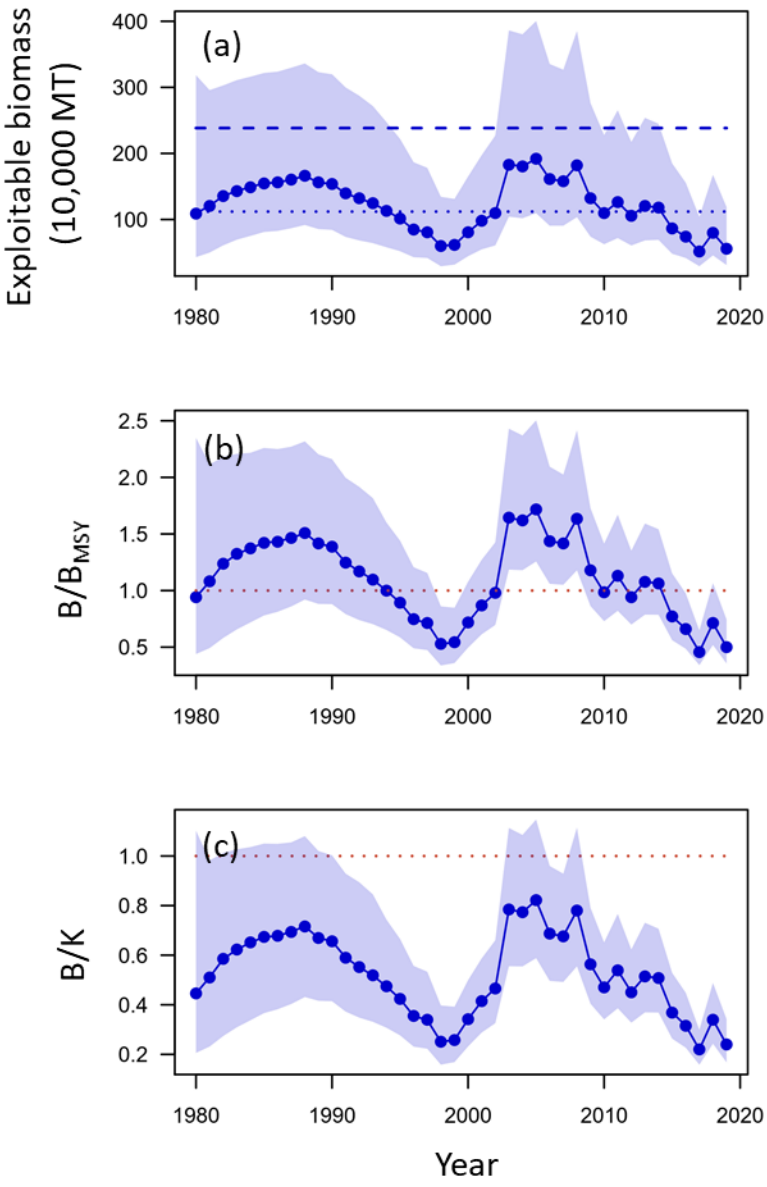

Figure S9. Time series of biomass (10,000 metric ton) (a), ratio of biomass to B_{MSY} (B/B_{MSY}) (b), and depletion ratio (B/K) of the Western North Pacific saury for the sensitivity case 2. In panel (a), the upper dashed and lower dotted horizontal line denotes the carrying capacity (K) and B_{MSY}, respectively. In panels (b) and (c), the dashed lines denote the reference levels of 1.

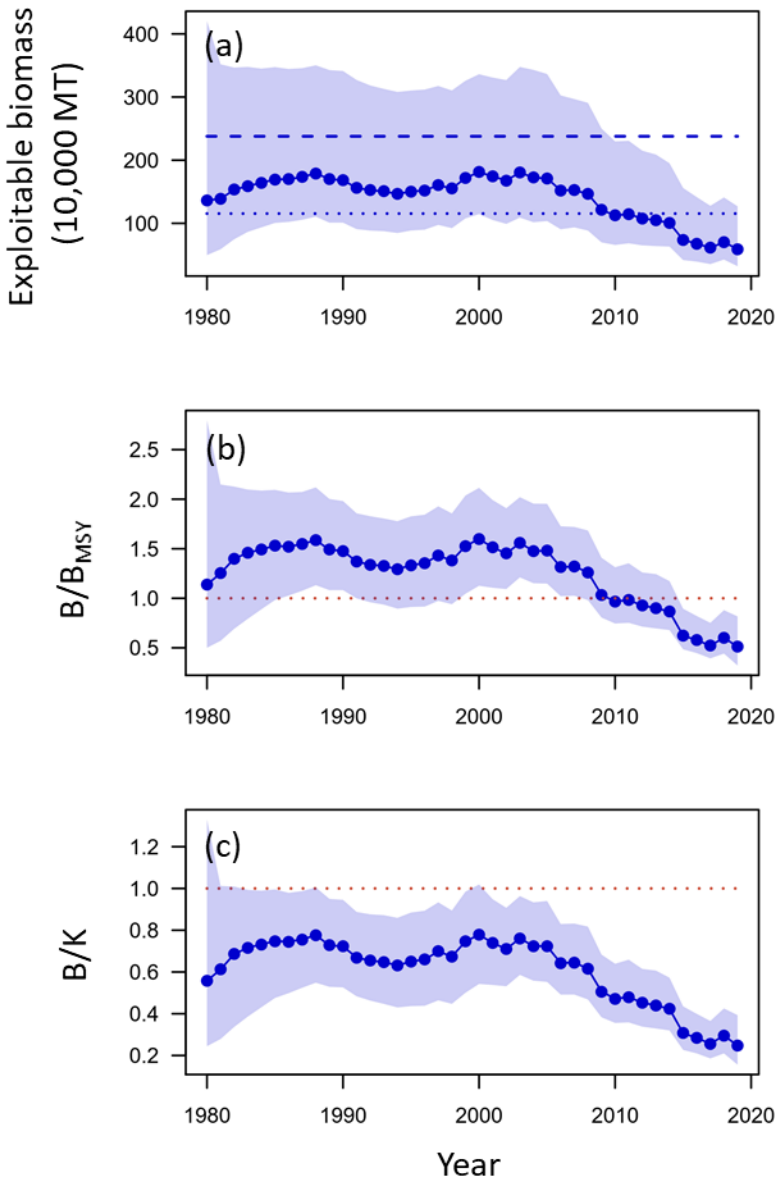

Figure S10. Time series of biomass (10,000 metric ton) (a), ratio of biomass to B_{MSY} (B/B_{MSY}) (b), and depletion ratio (B/K) of the Western North Pacific saury for the sensitivity case 3. In panel (a), the upper dashed and lower dotted horizontal line denotes the carrying capacity (K) and B_{MSY}, respectively. In panels (b) and (c), the dashed lines denote the reference levels of 1.

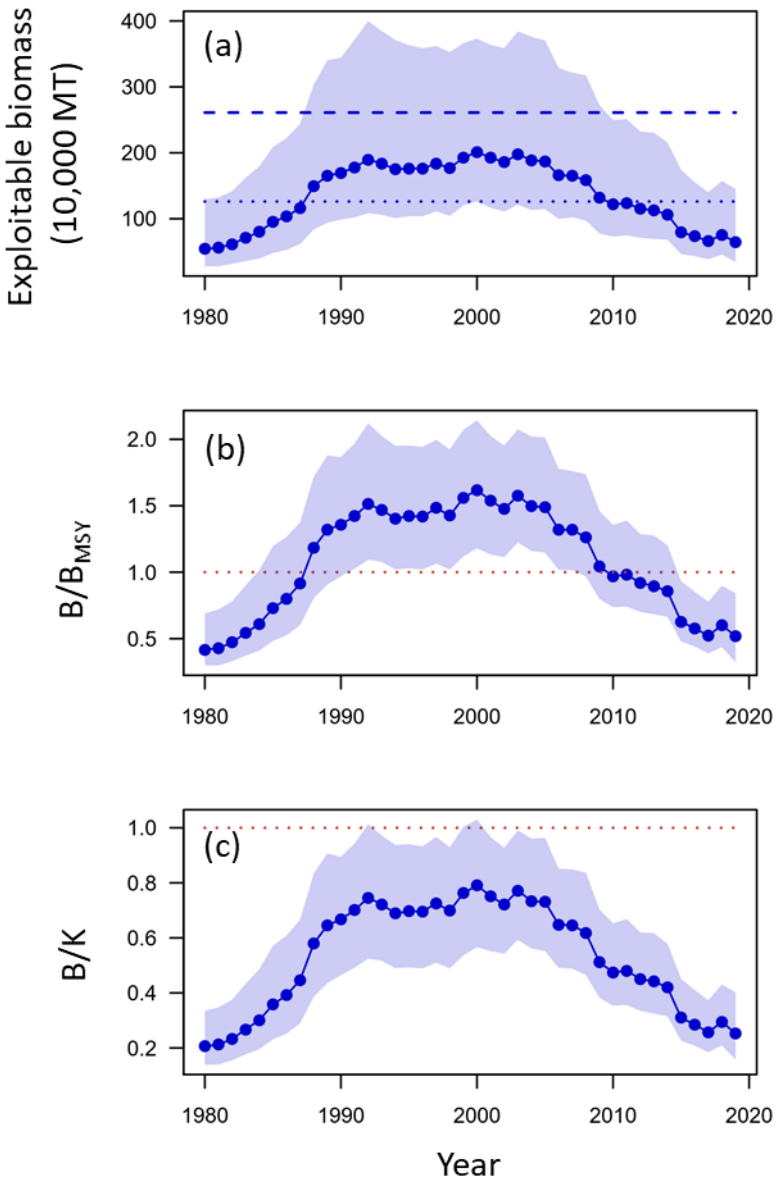

Figure S11. Time series of biomass (10,000 metric ton) (a), ratio of biomass to B_{MSY} (B/B_{MSY}) (b), and depletion ratio (B/K) of the Western North Pacific saury for the sensitivity case 4. In panel (a), the upper dashed and lower dotted horizontal line denotes the carrying capacity (K) and B_{MSY}, respectively. In panels (b) and (c), the dashed lines denote the reference levels of 1.

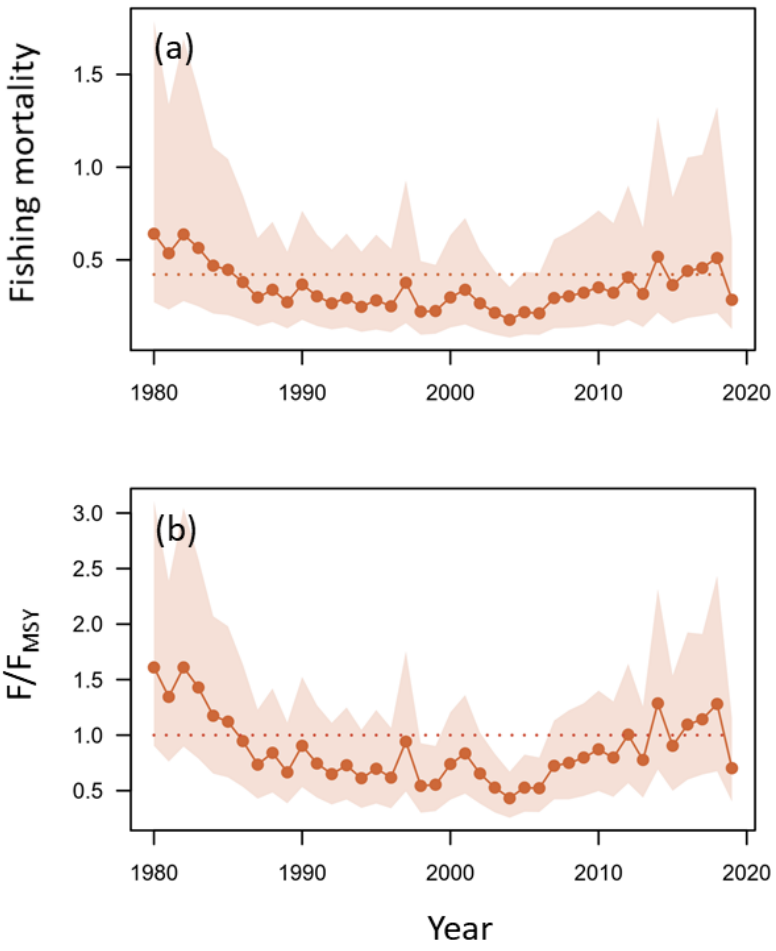

Figure S12. Time series of fishing mortality (a) and ratio of fishing mortality to F_{MSY} (F/F_{MSY}) (b) of the Western North Pacific saury for the base case 1. In panel (a), the dashed line denotes the F_{MSY}. In panels (b), the dashed line denotes the reference levels of 1.

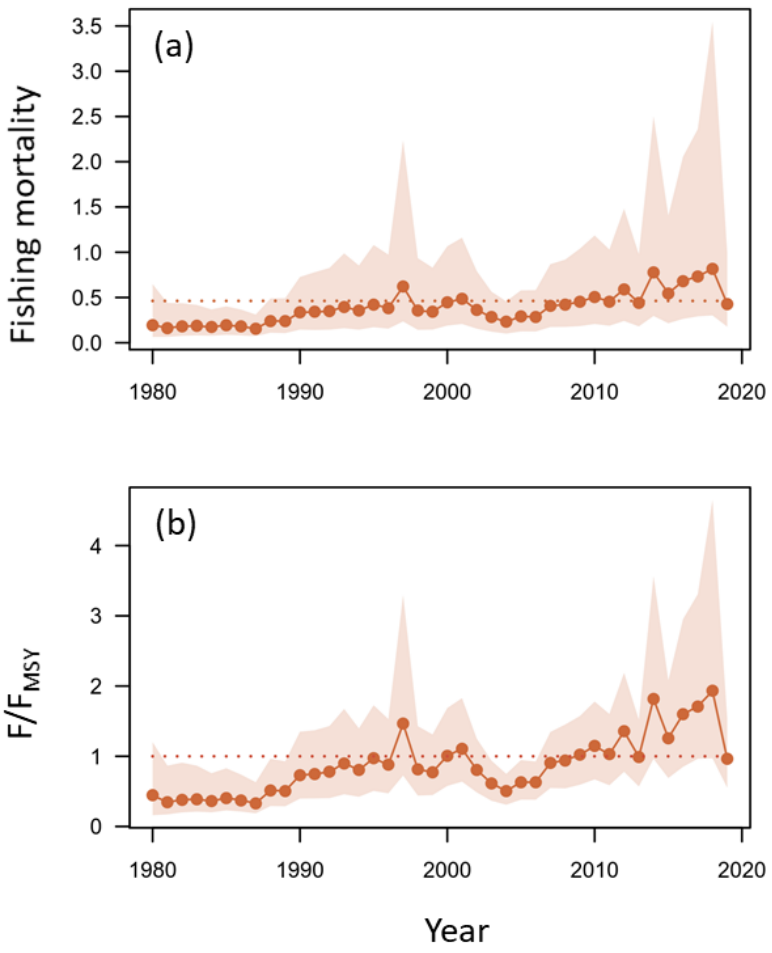

Figure S13. Time series of fishing mortality (a) and ratio of fishing mortality to F_{MSY} (F/F_{MSY}) (b) of the Western North Pacific saury for the base case 2. In panel (a), the dashed line denotes the F_{MSY}. In panels (b), the dashed line denotes the reference levels of 1.

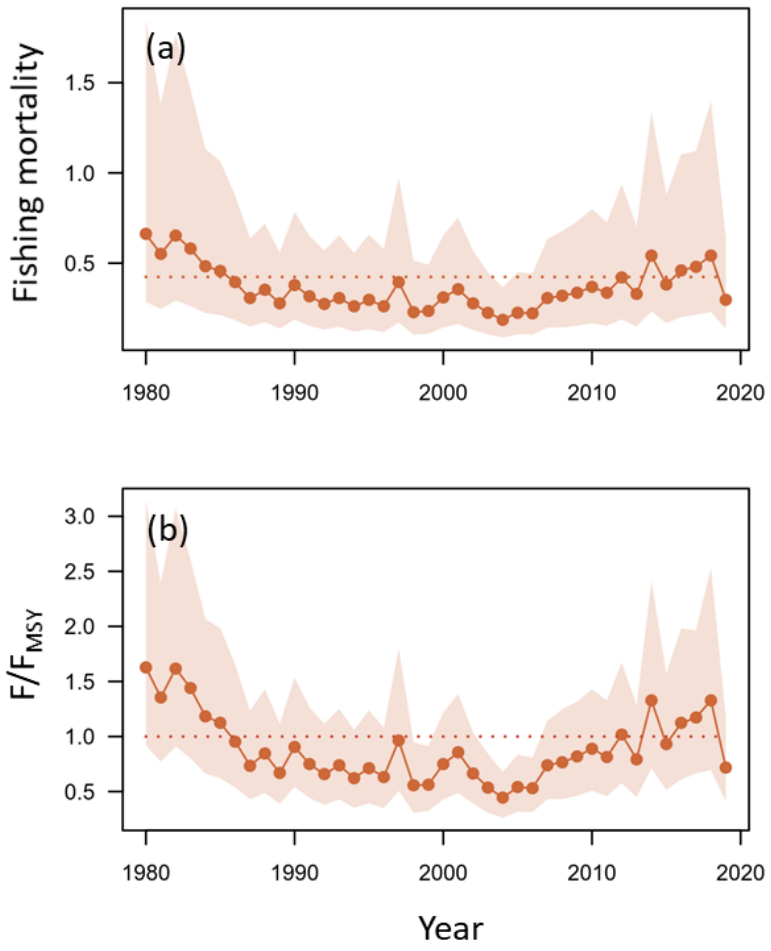

Figure S14. Time series of fishing mortality (a) and ratio of fishing mortality to F_{MSY} (F/F_{MSY}) (b) of the Western North Pacific saury for the sensitivity case 1. In panel (a), the dashed line denotes the F_{MSY}. In panels (b), the dashed line denotes the reference levels of 1.

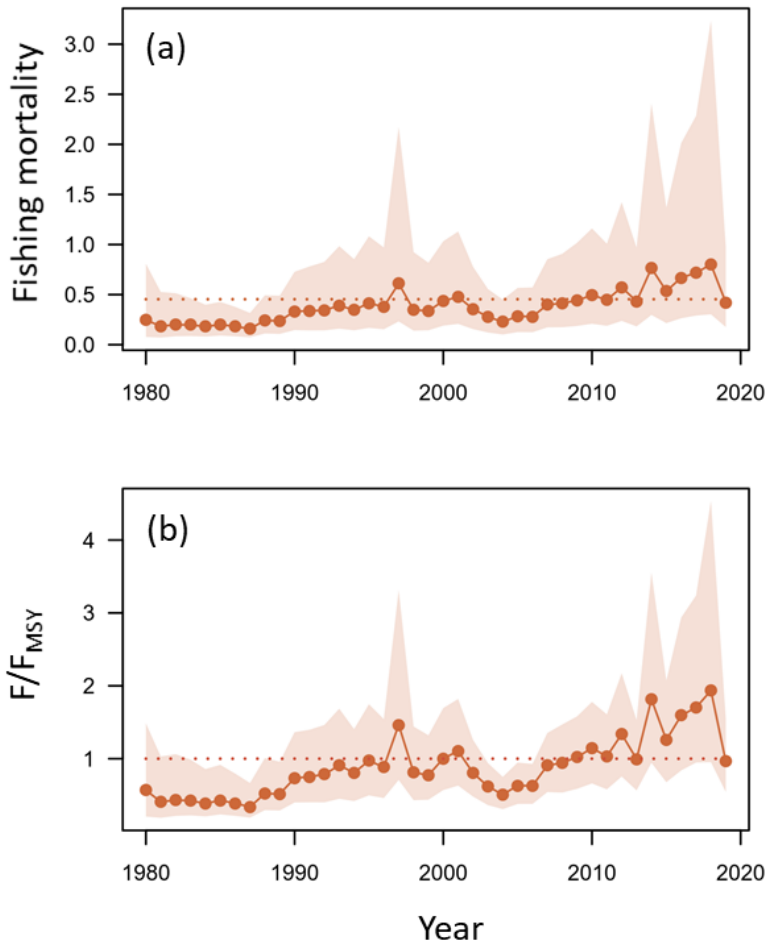

Figure S15. Time series of fishing mortality (a) and ratio of fishing mortality to F_{MSY} (F/F_{MSY}) (b) of the Western North Pacific saury for the sensitivity case 2. In panel (a), the dashed line denotes the F_{MSY}. In panels (b), the dashed line denotes the reference levels of 1.

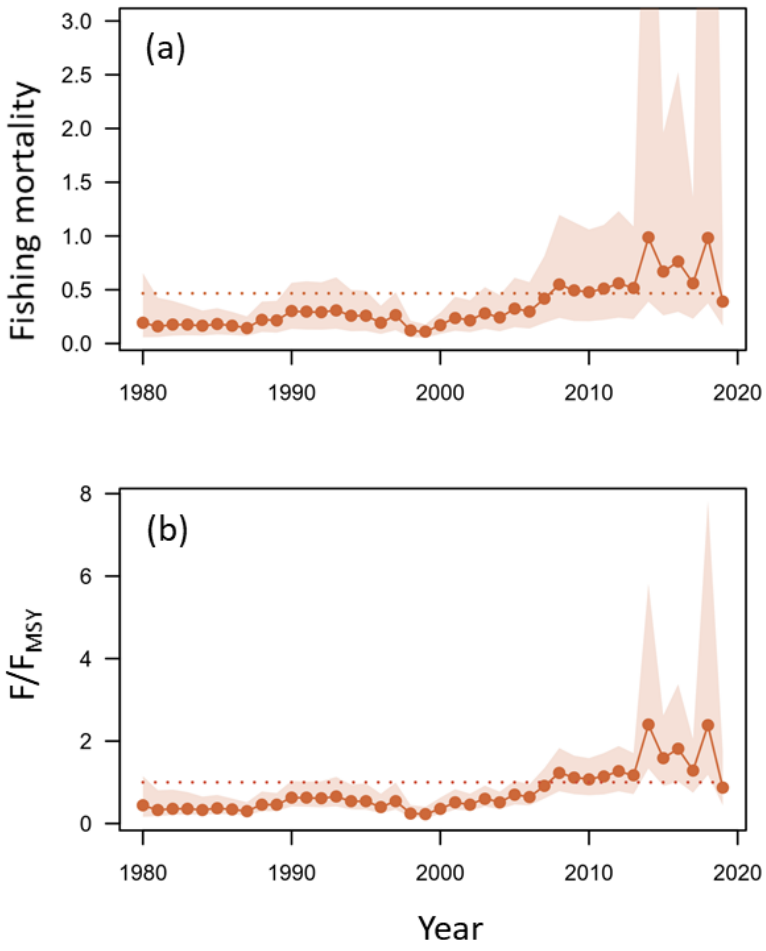

Figure S16. Time series of fishing mortality (a) and ratio of fishing mortality to F_{MSY} (F/F_{MSY}) (b) of the Western North Pacific saury for the sensitivity case 3. In panel (a), the dashed line denotes the F_{MSY}. In panels (b), the dashed line denotes the reference levels of 1.

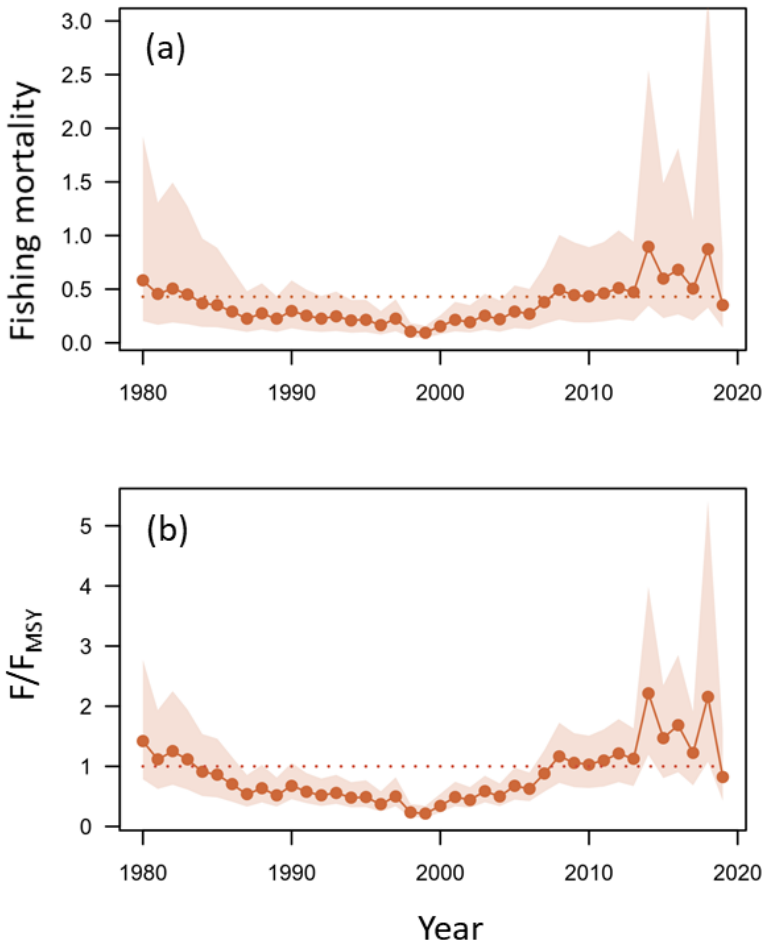

Figure S17. Time series of fishing mortality (a) and ratio of fishing mortality to F_{MSY} (F/F_{MSY}) (b) of the Western North Pacific saury for the sensitivity case 4. In panel (a), the dashed line denotes the F_{MSY}. In panels (b), the dashed line denotes the reference levels of 1.

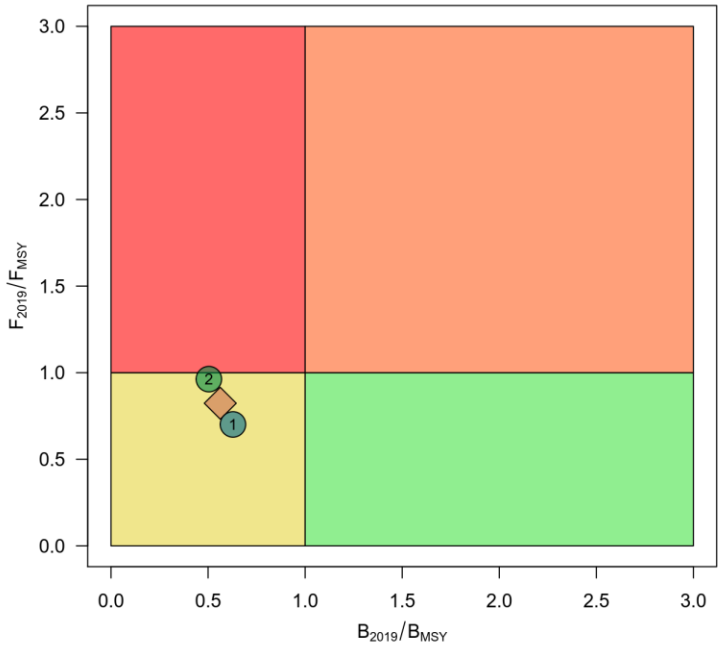

Figure S18. Kobe phase plot of stock status in 2019 of Pacific saury from the two base case models. The orange diamond is the median estimate of MCMC results from the two base case models.

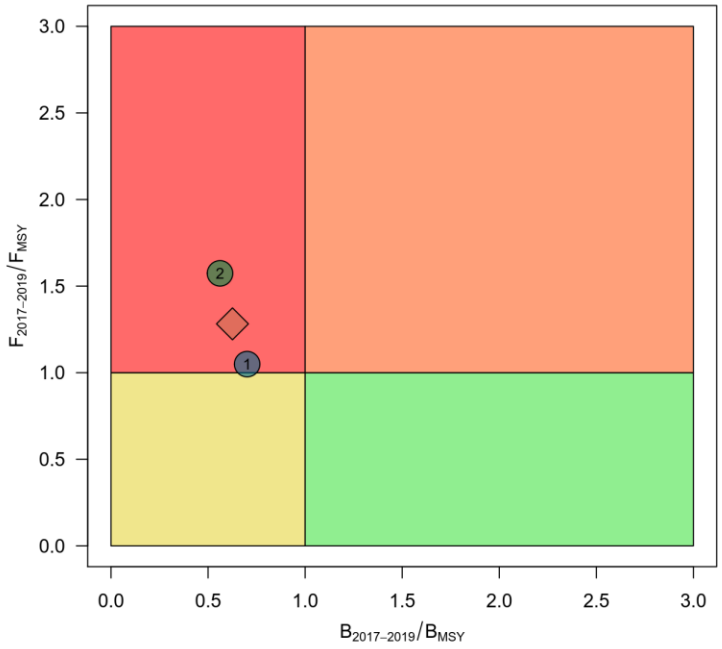

Figure S19. Kobe phase plot of average stock status ($B_{2017\text{-}2019}/B_{MSY}$ and $F_{2017\text{-}2019}/F_{MSY}$) of Pacific saury from the two base case models. The orange diamond is the median estimate of MCMC results from the two base case models.

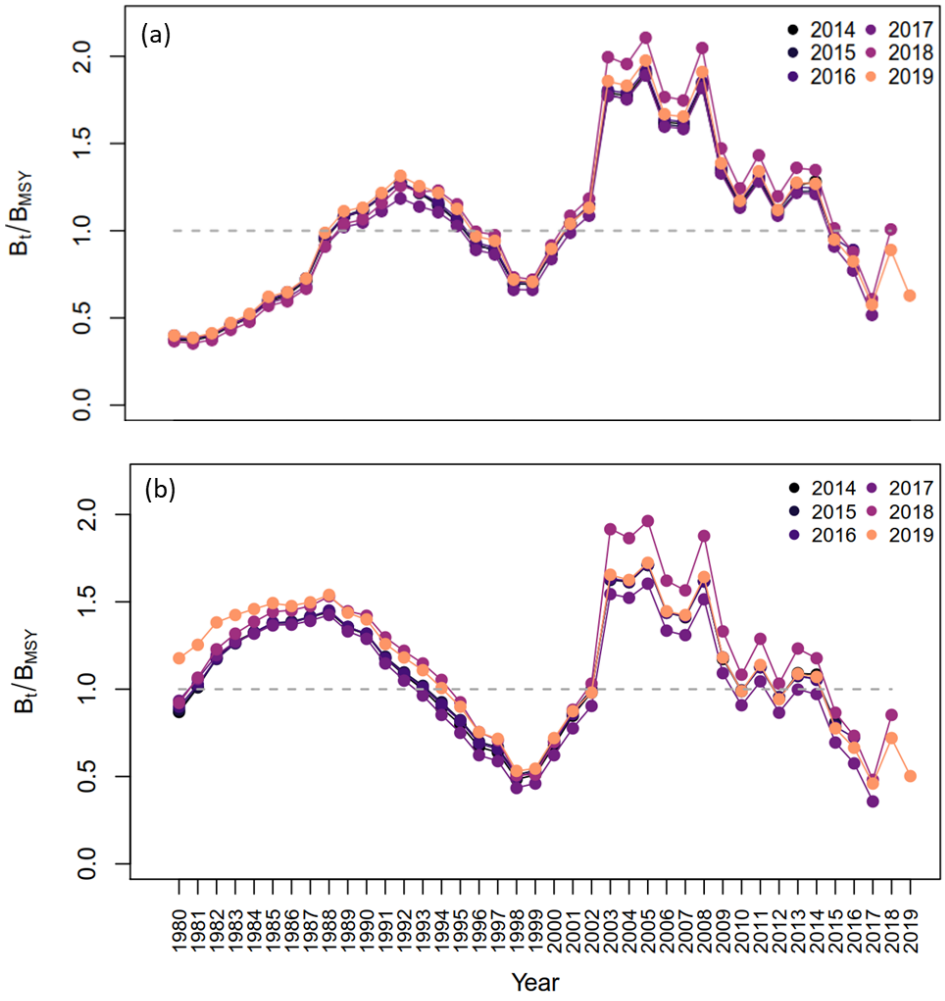

Figure S20. Six years within–model retrospective plots of the change in biomass to B_{MSY} of the Western North Pacific saury from the base case 1 (a) and 2 (b).

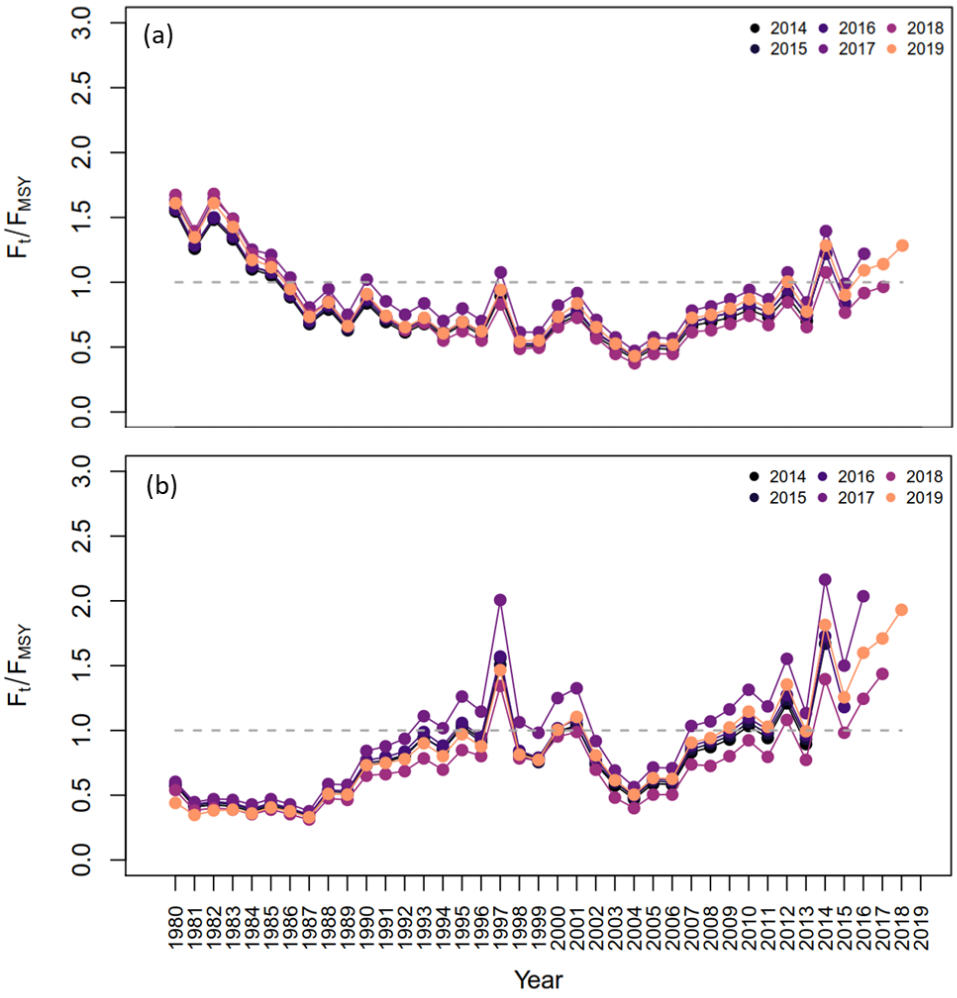

Figure S21. Six years within–model retrospective plots of the change in fishing mortality to F_{MSY} of the Western North Pacific saury from the base case 1 (a) and 2 (b).